

Original Article

Novel effect and the mechanistic insights of fruiting body extract of medicinal fungus *Antrodia cinnamomea* against T47D breast cancer



Kuang-Ming Shang^{a,1}, Tzu-Hsuan Su^{a,1}, Wai Leng Lee^b, Wen-Wei Hsiao^c, Ching-Yi Chiou^a, Bing-Ying Ho^a, Sheng-Yang Wang^d, Lie-Fen Shyur^{a,e,f,*}

^a Agricultural Biotechnology Research Center, Academia Sinica, Taipei, Taiwan

^b School of Science, Monash University Sunway Campus, Selangor, Malaysia

^c Experimental Forest, College of Bio-Resources and Agriculture, National Taiwan University, Taipei, Taiwan

^d Department of Forestry, National Chung Hsing University, Taichung, Taiwan

^e PhD Program in Translational Medicine, College of Medicine, Kaohsiung Medical University, Kaohsiung, Taiwan

^f Graduate Institute of Pharmacognosy, Taipei Medical University, Taipei, Taiwan

ARTICLE INFO

Article history:

Received 7 December 2015

Revised 26 October 2016

Accepted 6 November 2016

Keywords:

Antrodia cinnamomea

Tamoxifen

Anti-angiogenesis

ER+ T47D breast cancer

Dehydroeburicoic acid

ABSTRACT

Introduction: Tamoxifen, an anti-oestrogenic drug for estrogen receptor positive (ER+) breast cancer, was observed to stimulate tumor growth or drug resistance in patients. *Antrodia cinnamomea* (AC), a precious medicinal fungus has been traditionally used as a folk remedy for cancers in Asian countries. The objective of this study was to investigate the bioefficacy and the underlying molecular mechanisms of the AC fruiting bodies extracts (AC-3E) against human ER+ T47D breast cancer cells, and compare the effect with that of tamoxifen.

Methods: Cell proliferation, migration, TUNEL assay, western blotting, time-lapse confocal microscopy analyses, chorioallantoic membrane assay, and a xenograft BALB/c nude mouse system were used in this study. Chemical fingerprinting of AC-3E was established using LC-MS.

Results: AC-3E attenuated T47D breast cancer cell activity by deregulating the PI3K/Akt/mTOR signaling pathway and key cell-cycle mediators, and inducing apoptosis. AC-3E also effectively inhibited tube-like structures of endothelial cells, blood vessel branching and microvessel formation *ex vivo* and *in vivo*. Significant preventive and therapeutic effects against T47D mammary tumor growth of AC-3E was observed comparable or superior to tamoxifen treatment in xenograft BALB/c nude mice. Dehydroeburicoic acid (2) was characterized as the main chemical constituent in AC-3E against breast cancer.

Conclusion: This study suggests that AC-3E extracts can be employed as a double-barreled approach to treat human ER+ breast cancer by attacking both cancer cells and tumor-associated blood vessel cells.

© 2016 Elsevier GmbH. All rights reserved.

Introduction

Breast cancer is the most frequently diagnosed life-threatening cancer in women and the leading cause of cancer death among

women worldwide. Current cancer therapies, including endocrine therapy, chemotherapy, and targeted therapy, play an important role in the treatment of breast cancer; however, drug resistance, severe side effects, high recurrence rate, and metastases remain threats to breast cancer patients. Systemic tamoxifen (endocrine) treatment, for instance, was found to cause tamoxifen-stimulated tumor growth or drug resistance (Schafer et al., 2000). Due to the shortcomings of the current therapies, there is a pressing need for development of new therapeutic or preventive agents for breast cancer. Phytomedicines or phytoagents with novel molecular mechanisms provide one potential area for development.

Antrodia cinnamomea (AC) (known as Niu-Chang-Chih in Chinese medicine) is a precious medicinal fungus endemic to Taiwan that has been popularly used as a folk medicine for various disorders. Recently, the therapeutic effect of AC fruiting body against chronic alcohol consumption-induced liver damage in rats was

Abbreviations: Akt, protein kinase B; CAM, chorioallantoic membrane; COX-2, cyclooxygenase-2; ER, estrogen receptor; Jak1, Janus kinase 1; mTOR, mammalian target of rapamycin; MTT, 3-(4,5-dimethylthiazol-2-yl)-2,5-diphenyl tetrazolium bromide; PARP, poly ADP ribose polymerase; PI, propidium iodide; PI3K, phosphatidylinositol 3-kinase; Stat3, signal transducer and activator of transcription 3; Tam, tamoxifen citrate.

* Corresponding author at: Agricultural Biotechnology Research Center, Academia Sinica, No. 128, Sec. 2, Academia Road, Nankang, Taipei 115, Taiwan. Tel./Fax: +886 2 26515028.

E-mail addresses: lfshyur@ccvax.sinica.edu.tw, jaclyn@gate.sinica.edu.tw (L.-F. Shyur).

¹ Both authors contributed equally to this article.

<http://dx.doi.org/10.1016/j.phymed.2016.11.006>

0944-7113/© 2016 Elsevier GmbH. All rights reserved.

reported (Huang et al., 2010) and other hepatoprotective activities of fruiting body extracts or mycelium from solid or submerged cultivation have been reviewed (Ao et al., 2009; Geethangili and Tzeng, 2011). Also, AC extract has been shown to protect normal mouse spleen immune cells from radiation-mediated side effects, but intriguingly, the extract selectively enhanced radiation-induced inflammation and cytotoxicity in human colorectal cancer cells (Cheng et al., 2014).

Several reports on the anti-cancer activities of fruiting body extracts of *A. cinnamomea* have shown that total AC extracts prepared by organic solvents such as methanol, chloroform, ethanol or ethylacetate exhibit various anti-cancer activities against HepG2, PLC/PRF/5 liver cancer cells (Hsu et al., 2007), colon, Jurkat or prostate cancer cell lines (Rao et al., 2007), or leukemia HL60 cells (Hseu et al., 2004), through regulation of Bcl-2 family proteins, and activation of caspases or NF- κ B protein. In one recent study, programmed cell death via the autophagic pathway was observed in AC extract-treated head and neck cancer cells (Chang et al., 2013). A report of *A. cinnamomea* anti-human breast cancer cell activities focused on study of the fermented culture broth of AC against triple negative MDA-MB-231 cell activity (Yang et al., 2012b). The mode of action of these activities has been found to be through inhibition of the expression of COX-2 and induction of cell cycle arrest or apoptosis in MDA-MB-231 cells *in vitro* or in a xenograft mouse model (Hseu et al., 2008, 2007), or through inhibition of the MAPK signaling pathway (Yang et al., 2011). So far, only the fermented culture broth of AC has been reported to induce apoptosis in estrogen receptor positive (ER+) breast cancer MCF-7 cells (Yang et al., 2006). Little or no information concerning the bioactivity and mode of action of the fruiting body extracts of AC against ER+ breast cancer cells, such as T47D cells has been reported.

Because approximately 70% of breast cancer patients are diagnosed with ER+ cancer, and the current ER antagonistic drug (tamoxifen) shows drug resistance or side effects (Ring and Dowsett, 2004), this study aimed to investigate the pharmacological activity and the underlying modes of action of the fruiting body extract of *A. cinnamomea* against human ER+ T47D breast cancer cells. Further, to address the quality control of this folk medicine, the chemical fingerprint and active constituent(s) in the *A. cinnamomea* extract were also characterized.

Materials and methods

Cell lines and culture conditions

T47D, a human mammary ductal carcinoma cell line obtained from American Type Culture Collection, ATCC, Manassas, VA, USA, was grown in Roswell Park Memorial Institute 1640 medium (RPMI-1640; Life Technologies, Grand Island, NY, USA); H184B5F5/M10 (ATCC), a human mammary epithelial cell line, was cultured in minimum essential medium (MEM; Life Technologies, USA). All cell lines were cultured in specific media supplemented with 10% fetal bovine serum (FBS) and 100 U/ml penicillin in a humidified 5% CO₂ incubator at 37 °C.

Preparation of *Antordia cinnamomea* fruiting body extract

A. cinnamomea fungus was grown on the aromatic tree *Cinnamomum kanehirai* Hayata at the Experimental Forest Station, National Taiwan University and authenticated by Dr. Wen-Wei Hsiao. The fruiting bodies of *A. cinnamomea* were harvested at 3 months, 6 months, or 9 months, and designated AC-3, AC-6, and AC-9, respectively. The fruiting body samples were lyophilized and powdered using a pestle in liquid nitrogen. Fruiting body powder (10 g) of *A. cinnamomea* was extracted with ten times volume of 95% ethanol at room temperature for 3 h repeated twice. The

extracts were collected by centrifugation and the total ethanolic extracts (2.3 g, 1.9 g, and 1.5 g) designated AC-3E, AC-6E, and AC-9E were concentrated in a rotary evaporator and lyophilized.

Chemicals and reagents

Dimethyl sulfoxide (DMSO), tamoxifen citrate (Tam), 3-(4,5-cimethylthiazol-2-yl)-2,5-diphenyl tetrazolium bromide (MTT), propidium iodide (PI) and fibronectin were purchased from Sigma-Aldrich, St. Louis, MO, USA. Carboxymethylcellulose (CMC), Tween 20, primary antibodies against phosphatidylinositol 3-kinase (PI3K), protein kinase B (Akt), p-Akt, Janus kinase 1 (Jak1), signal transducer and activator of transcription 3 (Stat3), p38 MAPK, E-cadherin, poly ADP ribose polymerase (PARP) (Cell Signaling Technology, Danvers, MA, USA), actin, estrogen receptor alpha (ER α), mammalian target of rapamycin (mTOR) (Merck Millipore, Darmstadt, Germany), and p-p21 (Cayman Chemical, Ann Arbor, MI, USA) were used. All other antibodies in this study were from Santa Cruz Biotechnology, Dallas, TX, USA.

Experimental animals

Female BALB/c nude mice (4 weeks old) obtained from the National Laboratory Animal Center, Taipei, Taiwan were given a standard laboratory diet and distilled water *ad libitum* and kept on a 12 h light/dark cycle at 22 \pm 2 °C under specific pathogen-free conditions. All animal work was done in accordance with the protocol approved by the Institutional Animal Care and Use Committee (IACUC), Academia Sinica, Taiwan.

Cell proliferation assay

For the cell proliferation assay, T47D and M10 cells were seeded and grown in 96-well plates at 1 \times 10⁴ cells/well overnight. Cells were treated for 48 h with vehicle (0.5% DMSO or 0.5% ethanol), AC-3E, AC-6E, AC-9E or Tam. Cell viability was measured by MTT-based colorimetric assays (Huang et al., 2010).

Time-lapse microscopy analysis

Time-lapse microscopy analysis followed the procedure as previously reported (Lee and Shyur, 2012). T47D cells were seeded and allowed to adhere overnight in RPMI-1640 medium containing 10% FBS on a 60-mm-diameter culture plate coated with 10 μ g/ml fibronectin. AC-3E (50 μ g/ml), Tam (30 μ M) and vehicle were added at the beginning of time-lapse. The time-lapse experiments were conducted on an inverted Zeiss Axiovert 200 M microscope equipped with an environmental chamber with phase-contrast optics (images taken every 30 min). An average of 15 cells was randomly selected to calculate the distances cells migrated and the trajectories within 24 h, using the object-tracking application of Metamorph software (Molecular Devices, Sunnyvale, CA, USA).

Confocal microscopy

For F-actin staining, T47D cells were fixed with 4% paraformaldehyde after treatment with AC-3E or Tam. Cells were then permeabilized with PBS containing 0.2% Triton X-100, and rinsed with PBS. Fixed cells were incubated in buffer with rhodamine-phalloidin for 30 min. The nuclei were stained with DAPI. The cellular staining on actin in T47D cells was viewed and captured on a Zeiss LSM 510 META laser scanning confocal microscope.

Wound-healing assay

T47D cells were seeded in a two-side chamber at 1×10^6 cells/ml and allowed to adhere overnight. Chamber was removed and then treated with indicated concentrations of AC-3E. Photos were taken under microscopy every 24 h to observe the cell migration.

Transwell migration assay

T47D cells (1×10^5) were seeded into a transwell chamber (Merck Millipore, Darmstadt, Germany) containing serum-free medium and the indicated concentrations of AC-3E or Tam for migration assay. The chambers were put into a 24-well plate in which each well was covered with 500 μ l of medium containing 10% FBS, and incubated for 96 h. Cells on the upper surface of the chamber were scraped with a cotton swab, and the remaining cells were fixed and stained with DAPI (1 μ g/ml). Migrated cells in the lower surface of the chamber were counted at 100 \times magnification by inverted fluorescence microscopy.

TUNEL assay

T47D cells (3×10^4) were seeded and allowed to adhere overnight on a coverslip coated with 0.1% (w/v) poly-L-lysine (Sigma-Aldrich, St. Louis, MO, USA). Cells were treated with vehicle or AC-3E and Tam for 48 h. Cells were fixed using 4% formaldehyde/PBS at 4 °C for 25 min. After TdT enzyme reaction and PI staining (10 μ g/ml) following the DNA Fragmentation assay kit (ApoAlert, Clontech, Palo Alto, CA, USA), cover slips were sealed overnight in the dark. Apoptotic cells were visualized with green fluorescence using a standard fluorescence filter set (520 ± 20 nm). PI-stained cells exhibited red fluorescence when viewed at > 620 nm.

Endothelial cell proliferation assay

Early passages (< 5 passages) of primary human umbilical vein endothelium cell (HUVEC) were used for cell proliferation assays. HUVECs (1×10^4 cells/well) were seeded in a 96-well in EndoGRO-LS complete medium (Merck Millipore, Darmstadt, Germany). After 12 h, cells were treated for 48 h with vehicle (0.5% DMSO or 0.5% ethanol), AC-3E or Tam at indicated concentrations. Cell viability was measured by MTT-based colorimetric assays (Huang et al., 2010).

Tube formation assay

Fifty μ l growth factor-reduced matrigel (BD Bioscience, San Jose, CA, USA) was coated onto the pre-chilled 96-well plate on ice, and then being polymerized at room temperature for 1 h. A suspension of HUVEC (1×10^4 cells/well) in EndoGRO-LS complete medium (Merck Millipore, Darmstadt, Germany) was mixed with 1% FBS and with or without VEGF (100 ng/ml). The cells were treated with vehicle (0.5% DMSO or 0.5% ethanol), AC-3E, or Tam at indicated concentrations and times at 37 °C. The tube formation and drug effects were observed by light microscopy and pictures were taken at 100 \times magnification.

Western blot analysis

T47D cells (1×10^6) were grown in 10 cm dish overnight and starved in serum-free medium for 24 h. After treatment with AC-3E at different time points, proteins were harvested and resolved by 5–15% gradient SDS-PAGE, and electrophoretically transferred to PVDF membranes, which were then blocked in 3% w/v skimmed

milk with specific primary antibodies overnight (4 °C) and then incubated with secondary antibodies for 3 h at room temperature. Enhanced chemiluminescence detection reagents (ECL; Merck Millipore, Darmstadt, Germany) were used to visualize the positive reactive protein band by exposure to chemiluminescence light film.

Matrigel encapsulated chorioallantoic membrane(CAM) assay

Chick embryo CAM assays were performed by modification of a previously published method (Kim et al., 1998). Fertilized eggs were placed in an incubator as soon as embryogenesis started and kept under constant humidity at 37 °C. On the 7th day, a window was made under aseptic conditions on the eggshell. Aliquots (50 μ l) of Matrigel (BD Bioscience, San Jose, CA, USA) containing VEGF (50 ng/ml) supplemented with AC-3E or Tam at indicated concentration were mixed well on ice, pre-gelated at 37 °C, and then placed onto the CAM. The opening was closed with cellophane tape and incubation was continued until the day of the experiment. Capillary tube formation in the CAM was readily analyzed by the images taken at the 3rd day after grafting. The branching points of capillary blood vessels were quantified.

Inhibition of T47D tumor growth in BALB/c nude mice

All animal care and experimental procedures were approved by the Institutional Animal Care and Utilization Committee (IACUC; Protocol#: TMilBASL2010085) of Academia Sinica, Taipei, Taiwan, and reported in compliance with the Animal Research: Reporting In Vivo Experiments (ARRIVE) guidelines for reporting experiments involving animals. Mice were divided into groups of seven and were implanted with 17 β -estradiol pellets (0.72 mg, released over 60 days; American Innovative Research) one day before (day 1) the mammary fat pad region of mice was injected with T47D cells (5×10^6 cells/200 μ l PBS) (day 0). At day 7, the mice that carried tumors sized 48–55 mm³ were randomized and assigned into five groups. AC-3E and Tam were dissolved in vehicle (10% ethanol, 81% CMC and 9% Tween 20). AC-3E (50 mg/kg body weight, AC-3E-50; or 100 mg/kg body weight, AC-3-100) and Tam (30 mg/kg body weight, Tam-30) were given orally (*p.o.*) every other day starting on day 7 to day 33 (14 doses in total). Tam-30 and AC-3E-50 alternate treatment group was administered *p.o.* with Tam-30 on day 7 and then AC-3E-50 on day 9 in alternation for the following treatment days before the animal sacrificed on day 35 (7 doses of Tam-30 and 7 doses of AC-3E-50 in total). The PreAC-3E-50 group was *p.o.* pretreated with seven doses of AC-3E-50 before tumor cell implantation on day 7. The sham control and tumor control mice were *p.o.* with vehicle every other day. The tumor volume (*V*) was measured across two diameters with calipers every other day for five weeks and calculated by the formula $V = [(D + d)/2]^3$, where *D* and *d* were the larger and smaller diameters, respectively (Chung et al., 2006). At the end of the study, mice were killed by cervical dislocation. Tumors were removed, fixed with 10% buffered formalin, embedded in paraffin, and then examined visually and microscopically for growth of tumor cells. Tumor specimens were collected and subjected to pathological and immunohistochemical examinations.

Identification of index compounds

The total ethanolic AC-3 extract was separated by HPLC using the Agilent 1100 HPLC system equipped with a UV detector. A Luna RP C18 column (250 \times 4.6 mm; Phenomenex, Torrance, CA, USA) was employed with three solvent systems, H₂O (A), MeOH (B) and acetonitrile (C). The gradient elution profile was as follows: 0–5 min, A: B: C = 40:30:30 (isocratic); 5–95 min,

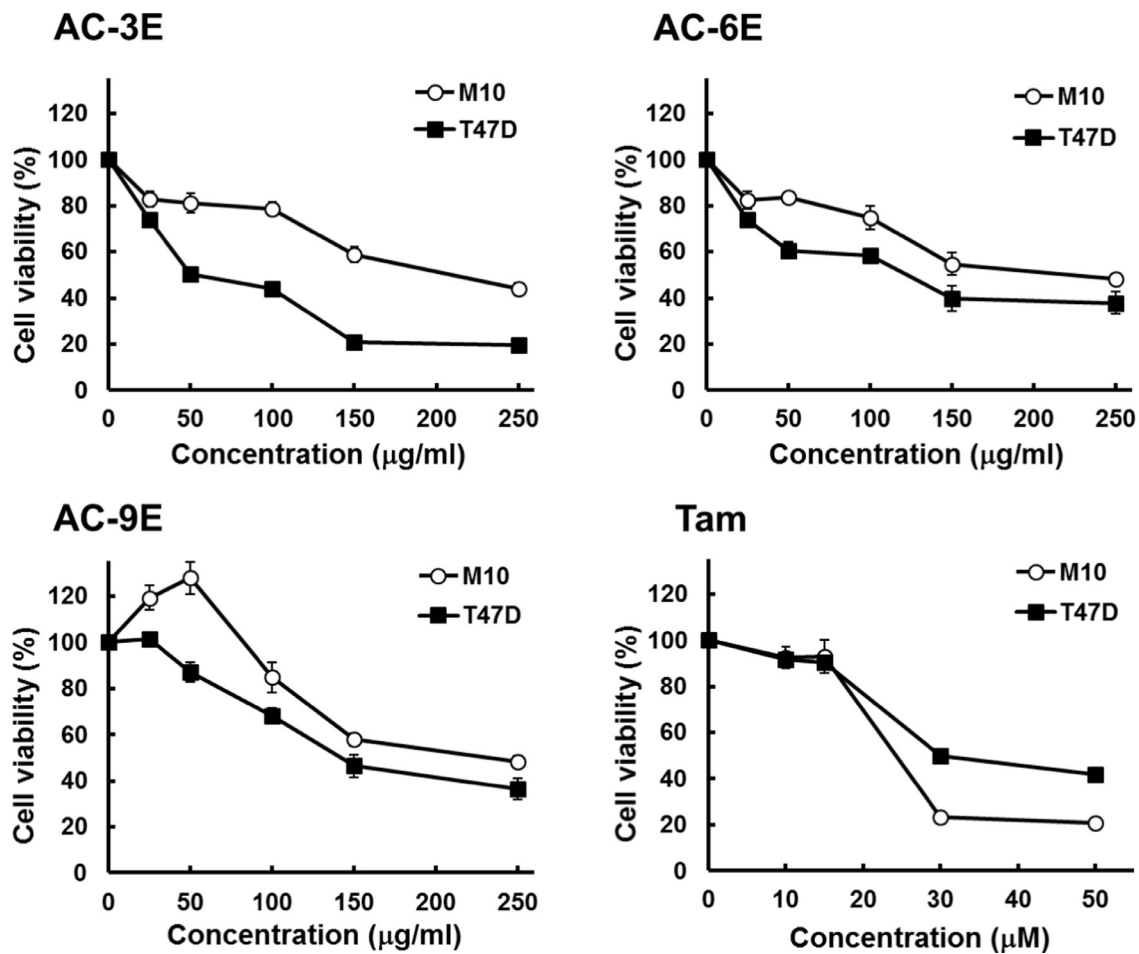


Fig. 1. Cell viability of T47D and M10 cells treated with AC-3E, AC-6E, AC-9E, or Tam at indicated concentrations. Data are expressed as mean \pm SD. Each value is the mean of at least three independent experiments.

A: B: C = 40:30:30 to A: B: C = 10:10:80 (linear gradient); 95–105 min, A: B: C = 10:10:80 to A: B: C = 0:0:100 (linear gradient); 105–115 min, 100% C (isocratic); the flow rate was 0.5 ml/min at 0–95 min; 1.0 ml/min at 95–115 min; and the detector wavelength was set at 254 nm. The structures of two major compounds, namely dehydrosulfurenic acid (1) and dehydroeburicoic acid (2) were elucidated using various spectral analyses and also confirmed with a previously published article (Lin et al., 2011).

Standard calibration curves (peak area vs. concentration) of the two candidate index compounds, dehydrosulfurenic acid and dehydroeburicoic acid were obtained at a range of compound concentrations, 25, 50, 100, 250, 500 and 1000 µg/ml. The peak area of the two compounds in the chromatogram of AC-3 extract (1 mg/ml) was defined by HPLC analysis, and their contents in the extract were calculated based on the quantity calibrated from the respective standard calibration curves.

Statistical analysis

Data are all expressed as mean \pm standard deviation. ANOVA was used to determine the significant differences between different conditions. $P < 0.05$ was considered statistically significant.

Results

AC-3 extract inhibits T47D cell proliferation

The anti-cancer cell proliferation activity on T47D (ER+) cells of the fruiting body extracts of *A. cinnamomea* grown for 3 months

(AC-3E), 6 months (AC-6E), or 9 months (AC-9E) was compared using MTT assay. Tamoxifen (Tam), an estrogen antagonistic drug, was used as a reference control in this study. The result in Fig. 1 shows that, at 48 h treatment, the magnitude of cell cytotoxicity against T47D cells is AC-3E > AC-6E > AC-9E, with an IC₅₀ of 52.7 µg/ml, 122.6 µg/ml, 141.9 µg/ml, respectively. Furthermore, AC-3E was less toxic to the normal human mammary epithelial cell line M10 than AC-6E and AC-9E at its IC₅₀ value for T47D. The IC₅₀ for Tam treatment of T47D cells was 30 µM; however, Tam was more toxic to normal mammary cells M10 at 24 µM. As AC-3E was the least toxic, hereafter, this study focused on investigating the anti-T47D breast cancer effects of AC-3E.

AC-3E attenuates T47D cell migration

Time-lapse microscopy was used to capture the kinetic characteristics of T47D cell morphological changes, proliferation, and migration under treatment with vehicle (0.5% DMSO), AC-3E (50 µg/ml), or Tam (30 µM) for 24 h. The images were continuously captured from 0 to 24 h and the representative images taken every 4 h are shown in Fig. 2. The AC-3E- and Tam-treated cells showed apoptotic rounded shapes and no further proliferation was observed compared to the vehicle-treated cells (Fig. 2A). Typical cell cytokinesis was captured at 12 h in vehicle-treated T47D cells, but not in the AC-3E or Tam-treated cells. Trajectories of T47D cell migration within 24 h under different treatments were monitored. The most significant cell dispersion area was seen in the vehicle-treated cells, and a relatively small and restricted area was revealed in AC-3E or Tam-treated cells (Fig. 2B). Consistent

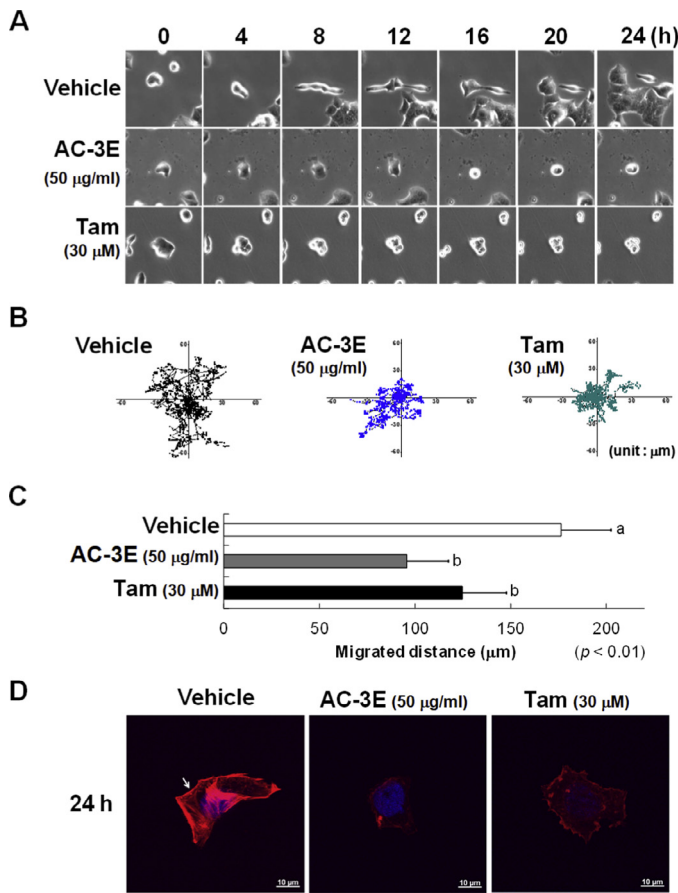


Fig. 2. Kinetic characteristics of T47D cell proliferation and motility in the presence of AC-3E and Tam. Video frames of representative cells were taken by time-lapse microscopy (A). Fifteen cells were randomly chosen to monitor the cell trajectories (B) and migration distances (C). Immunofluorescence confocal microscopy (D). $P < 0.01$ was considered statistically significant.

with the observation of cell trajectories, the migration distances of T47D cells were shorter with AC-3E (92 μm ; $P < 0.05$) and Tam (120 μm ; $P < 0.05$) treatment than with vehicle-treated (172 μm) cells (Fig. 2C).

Confocal microscopy coupled with immunofluorescent staining with actin was employed to observe the dynamics of stress fiber formation in T47D cells. In comparison with control cells, fluorescence intensity (red) indicated that polymerized actin was greatly reduced in AC-3E and Tam-treated cells (Fig. 2D). Therefore, the deleterious effect on T47D cell migration may be due to stress fiber formation by AC-3E or Tam treatment.

The horizontal and vertical migration of cancer cells is important for metastasis. The Boyden transwell migration assay revealed that AC-3E at 10 and 25 $\mu\text{g/ml}$ and Tam at 15 μM inhibited migration of T47D cells (Fig. 3A). Furthermore, AC-3E and Tam also significantly inhibited T47D cell migration as shown in the wound-healing assay (Fig. 3B). These results suggest that AC-3E may reduce the ability of T47D cells to invade basement membrane barriers.

AC-3E induces DNA damage and apoptosis in T47D cells

Induction of cell and DNA damage in T47D cells was investigated using TUNEL assay and PI staining. Fig. 4 shows that AC-3E dose-dependently increased DNA and cell damage as revealed by positively TUNEL stained (green fluorescein-dUTP) and PI stained (red FITC) cells with 48 h treatment with AC-3E, suggesting that

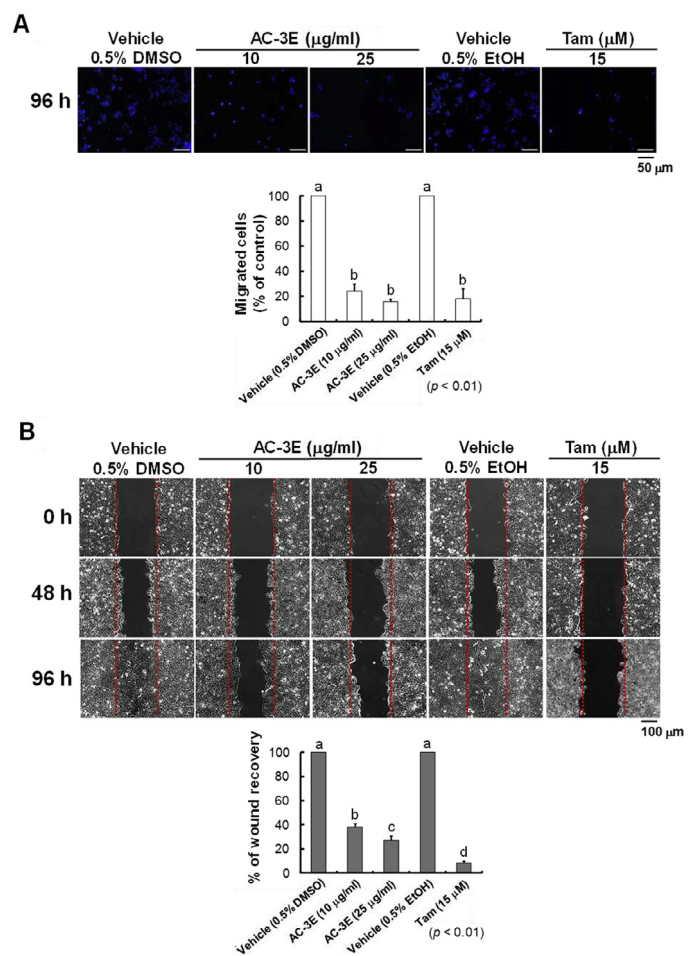


Fig. 3. Effect of AC-3E against T47D cell migration examined by Boyden transwell assay (A) and wound-healing assay (B).

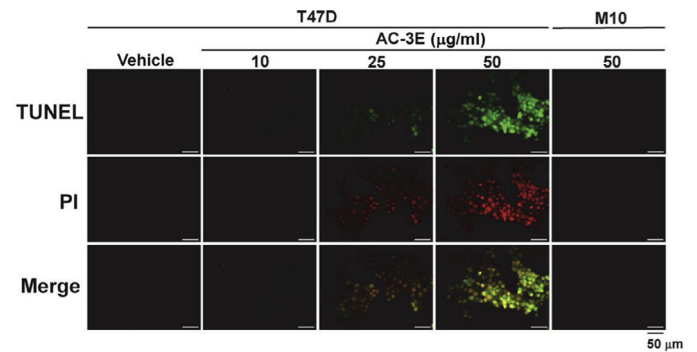


Fig. 4. TUNEL assay and PI-staining of T47D cells treated with indicated concentrations of AC-3E or Tam.

AC-3E caused apoptosis in T47D cells. In contrast, AC-3E did not cause M10 cell damage at high concentration (50 μM) treatment as no fluorescence intensity was detected.

AC-3E attenuates cell proliferation and VEGF-induced tube formation in HUVECs

The cell viability assay was first conducted to examine the potential toxicity of AC-3E and Tam against HUVEC cells. As shown in Fig. 5A, the IC_{50} of HUVEC cells under 48-h treatment of AC-3E and Tam are approximately of 2 $\mu\text{g/ml}$ and 5 μM , respectively. Further verifying the effect of AC-3E and Tam against VEGF-induced

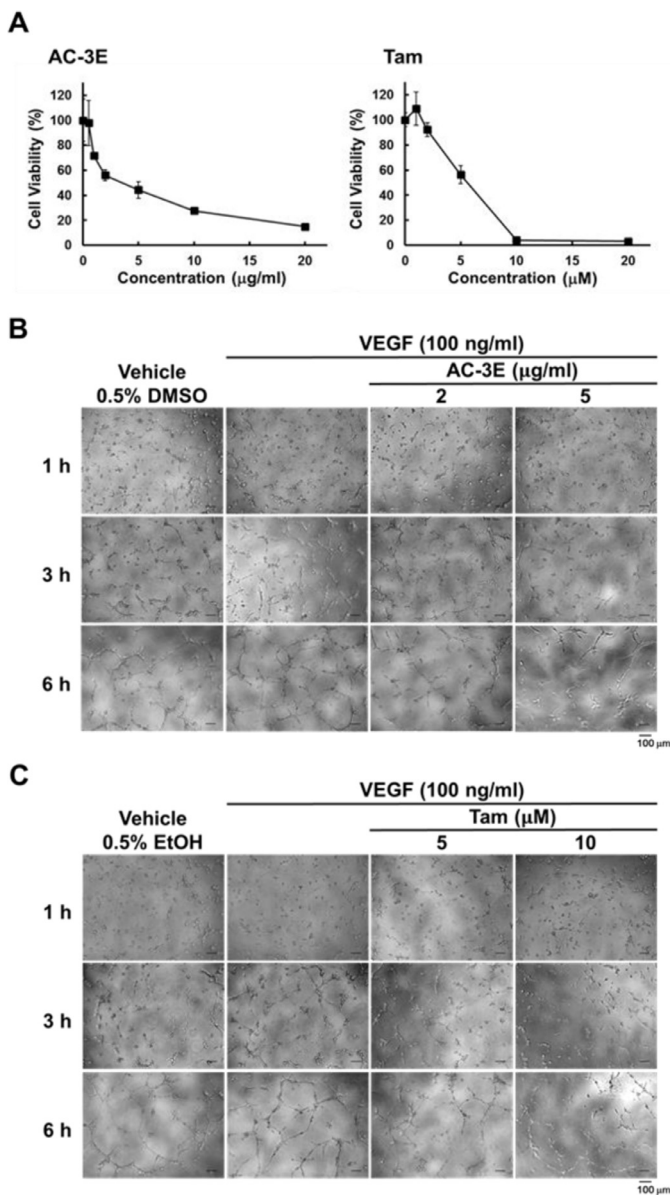


Fig. 5. (A) Cell viability of HUVEC cells treated with AC-3E or Tam at indicated concentrations and times. Data are expressed as mean \pm SD. Each value is the mean of at least three independent experiments. Inhibitory effect of AC-3E (B) and Tam (C) on tube formation of HUVEC cells stimulated by VEGF (100 ng/ml).

tube formation in HUVEC cells, we observed phenotypically less capillary-like and branches of tube morphology in the AC-3E and Tam treated HUVEC cells, indicating an inhibitory effect on the tube formation time- and dose-dependently as compared to the VEGF-treated only ones (Fig. 5B and C).

AC-3E modulates protein expression of cell-cycle mediators, actin dynamics mediators, E-cadherin and β -catenin

Western blot analysis showed that AC-3E at 50 μ g/ml inhibited the protein expression of several cell cycle mediators, including Cdk 4, Cdk 6, cyclin B1, cyclin D3, Rb, and p-Rb in a time-dependent manner (Fig. 6A), indicating that cell cycle machinery in T47D cells was disturbed by AC-3E treatment.

Fig. 6B reveals that the protein expression of Rac1 and RhoA, two of the small Rho GTPase proteins involved in mediating actin dynamics in motile cells and during cell morphogenesis (Hall and Nobes, 2000) were inhibited. In addition, E-cadherin,

functioning as an invasion suppressor and β -catenin protein, an oncoprotein, were observed to be time dependently up-regulated and down-regulated, respectively, in AC-3E-treated cells (Fig. 6B).

AC-3E regulates key proteins involved in cell growth, proliferation, apoptosis, or inflammation

Overactivation of the PI3K/Akt/mTOR pathway has been reported to reduce cancer cell apoptosis and allow proliferation in cancer cells (Carraway and Hidalgo, 2004). A previous study also suggested that estrogen through the ER induces cell survival by activating the PI3K/Akt pathway (Ahmad et al., 1999; Bratton et al., 2010). In this study, western blotting results show that the protein levels of ER α , and key molecules involved in the PI3K/Akt pathway, such as PI3K, p-Akt, Akt, mTOR, MDM2 were all suppressed in AC-3E-treated cells time dependently compared to the vehicle control cells (Fig. 6C). Moreover, Jak1, Stat3, NF- κ B, p38 and COX-2 proteins that are involved in cell inflammation and carcinogenesis were also deregulated by AC-3E in T47D cells.

AC-3E inhibits ex vivo CAM angiogenesis

Next, Matrigel encapsulated CAM assay was employed to investigate whether AC-3E can inhibit blood microvessel formation. As shown in Fig. 7, VEGF induced branching of blood vessels and increased microvessel formation in the vehicle control. AC-3E and Tam dose-dependently reduced the number of branching blood vessels ($P < 0.05$) (Fig. 7), indicating both AC-3E and Tam possess anti-angiogenic activity.

AC-3E suppresses T47D mammary tumor growth in a xenograft mouse model with reduction of proliferation, angiogenesis and macrophage infiltration

We compared the AC-3E, Tam, and Tam and AC-3E alternate treatment effect on cancer prevention or therapeutic efficacy in BALB/c nude mice. The experimental design and protocol for evaluating the *in vivo* anti-breast cancer effect of AC-3E is shown in Fig. 8A. Mice were pretreated *p.o.* with 50 mg/kg AC-3E (PreAC-3E-50) for 7 days before tumor cell implantation on day 0, or administered *p.o.* with 50 or 100 mg/kg AC-3E (AC-3E-50 and AC-3E-100), 30 mg/kg Tam (Tam-30), or Tam-30 and AC-3E-50 alternate treatment (Tam-30&AC-3E-50) every two days until the end of the experiments at day 35. The mean tumor volume ($n=6$) was significantly reduced without showing deleterious effects on mouse body weight in all test groups (Fig. 8B–D). The inhibition (%) of tumor size was 90%, 89%, 81%, 80%, 75%, respectively, in AC-3E-100, PreAC-3E-50, AC-3E-50, Tam-30, and Tam-30&AC-3E-50 groups, as compared to the tumor control group. The data demonstrate that AC-3E has a comparable or superior effect to that of tamoxifen on suppressing T47D mammary tumor growth.

Immunohistochemical staining results showed that the proliferation index Ki67, endothelial cell marker CD31, and macrophage marker F4/80 were all significantly reduced in test mice (Fig. 8E), indicating that AC-3E treatment suppressed T47D cell proliferation, tumor angiogenesis, and macrophage infiltration.

Chemical fingerprinting of AC-3E and identification of major bioactive compounds

HPLC and various spectral analyses were employed to establish the chemical fingerprints of the bioactive AC-3E and to elucidate chemical structure of the major chemical constituents present in the extract. As shown in Fig. 9A, two major compound peaks are seen in the LC profile separated using a RP C18 HPLC column and the structure and name of both compounds were elucidated as

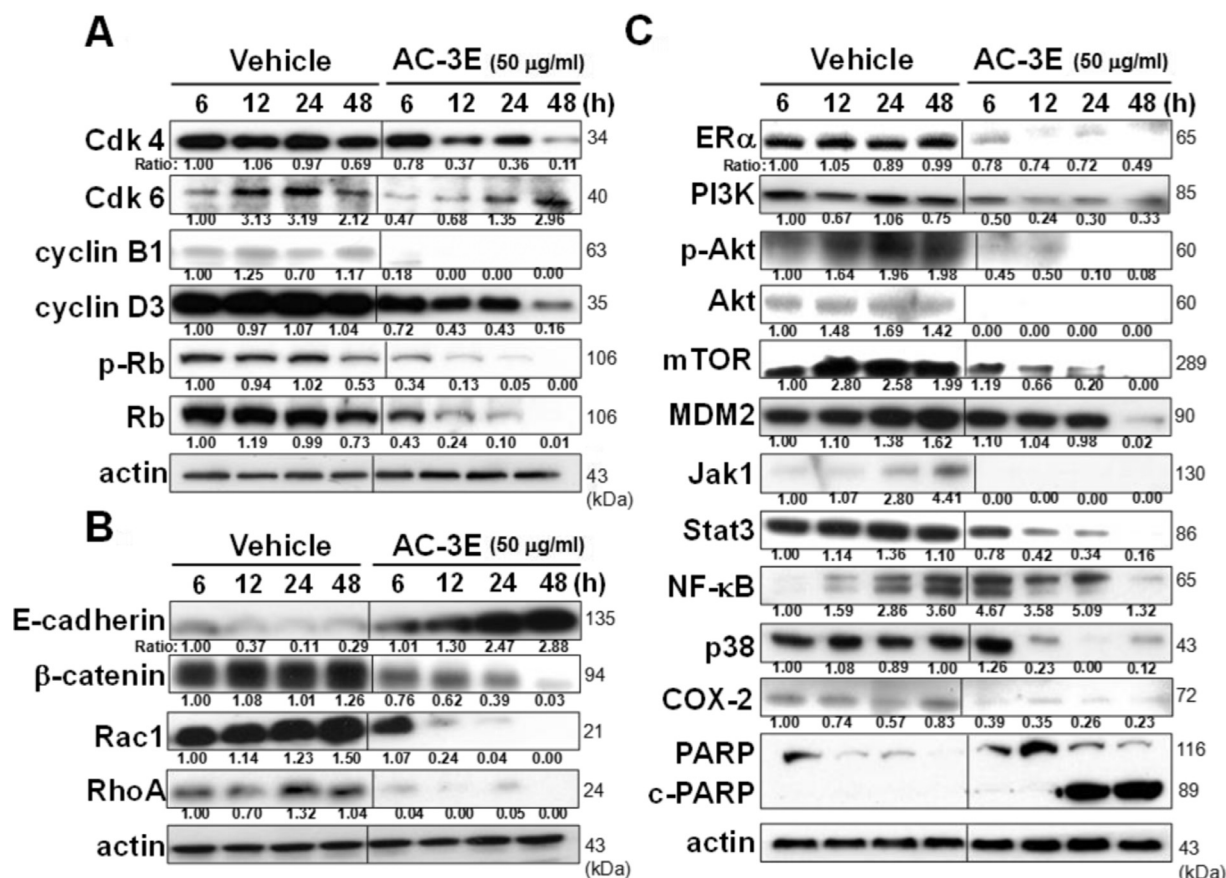


Fig. 6. Western blot analysis of protein expression profile related to cell-cycle mediation (A), cell migration (B), and cell growth, proliferation, and apoptosis (C) in AC-3E-treated T47D cells.

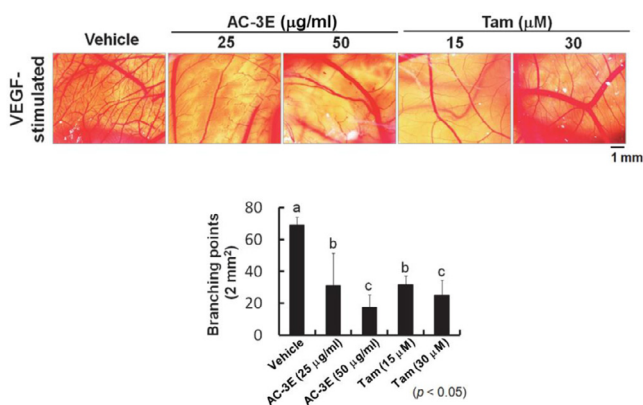


Fig. 7. Examination of the anti-angiogenesis effect of AC-3 using chorioallantoic membrane (CAM) assay. Five eggs in each treatment group were carried out in this experiment. Representative images of capillary tube formation in the CAM experiment of each treatment groups were shown. The branching points of blood microvessels were quantified and compared by ANOVA (*P* < 0.05).

dehydrosulfurenic acid (**1**) and dehydroeburicoic acid (**2**). The content of compound **1** and **2** in AC-3E was determined as 42.4% and 41.7%, respectively, by the respective calibration curves established in this study.

The cytotoxic effects of dehydrosulfurenic acid (**1**) and dehydroeburicoic acid (**2**) on T47D and M10 cell lines were further examined using MTT assay. The results in Fig. 9B demonstrate that compound **1** did not have a toxic effect on either breast cancer cells or normal cell lines, whereas, compound **2** exerted similar

anti-T47D cell activity to that of AC-3E, with little toxic effect on M10 cells. These results indicate that dehydroeburicoic acid (**2**) is the major bioactive compound in AC-3 extracts.

Discussion

In this study, *A. cinnamomea* fruiting body extracts were shown to attenuate proliferation, migration, and tumor growth of estrogen receptor positive T47D human breast cancer cells *in vitro* and *in vivo* by deregulating the PI3K/Akt signaling pathway and cell-cycle mediators, inducing apoptosis, and inhibiting tumor angiogenesis. This is the first report to demonstrate that AC extracts exert similarly potent activity to that of the standard estrogen antagonism drug tamoxifen against estrogen receptor-dependent T47D breast cancer cells.

We observed that AC-3E could significantly attenuate T47D migration through live video microscopy monitoring, wound healing and transwell invasion assay (Figs. 2 and 3). The anti-T47D cell migration effect of AC-3E is likely through deregulation of actin remodeling by the Rho GTPases, RhoA and Rac1 (Sepp and Auld, 2003), on the basis of our confocal microscopy and western blotting results (Figs. 2 and 6). Studies indicate that AC fruiting-body extract suppressed lung adenocarcinoma cell migration via inhibiting the PI3K/Akt signaling pathway (Chen et al., 2012). In fact, PI3Ks and Rho GTPases are both involved in cell polarization, motility, and chemotaxis. A network of Ras and Rho family small GTPases that induces and reinforces PI3K activity was recently proposed (Yang et al., 2012b).

The PI3K/Akt signaling pathway is also known to be involved in cell proliferation. When PI3K is activated, the expression of Akt is increased, which causes apoptosis resistance or cell cycle

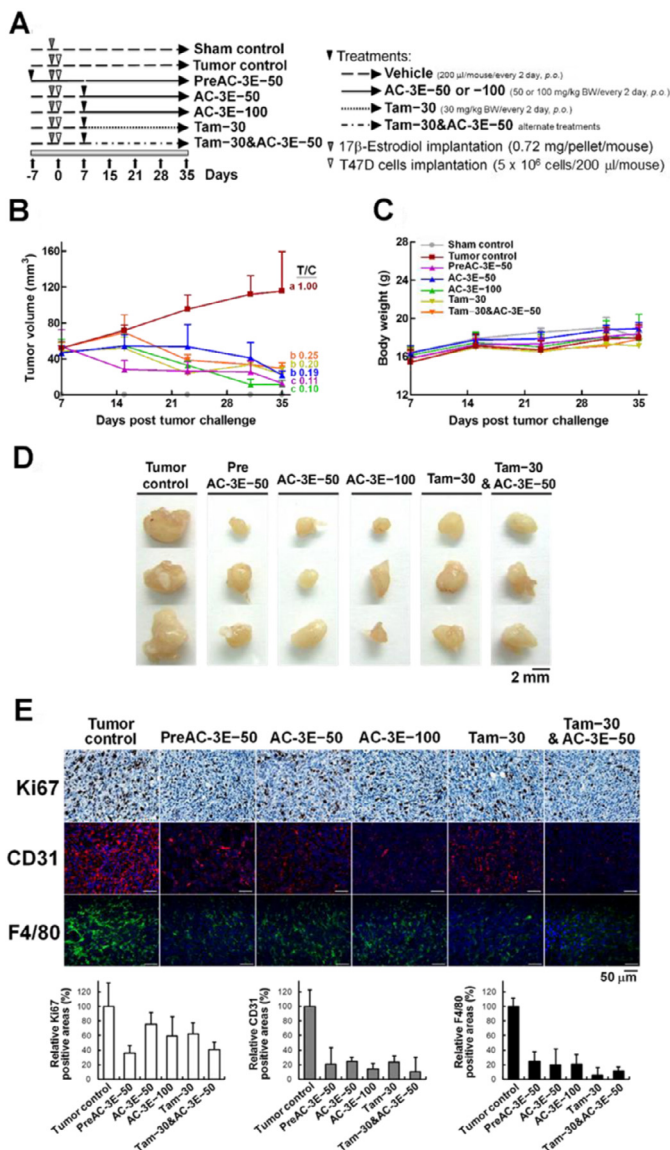


Fig. 8. Effects of AC-3E and Tam on the growth of breast tumors in a T47D xenograft model. Each group contained six BALB/c female nude mice with an average body weight of 16 g. (A) Experimental design and protocol. (B) Tumor growth curve and volume in each treatment group. Treatment-to-control (T/C) ratio is shown. (C) Mean body weight of each treatment group. (D) Representative photograph of dissected tumors of all tested groups. (E) Representative images of immunohistochemical staining of tumor specimen with Ki67, CD31, and F4/80: positive Ki67 (brown), positive CD31 (red), positive F4/80 (green), and DAPI staining for nucleus (blue). (For interpretation of the references to colour in this figure legend, the reader is referred to the web version of this article.)

promotion. A previous study also indicated that ER α can induce estrogen dependent MCF-7 cell survival through activating the PI3K/Akt pathway (Bratton et al., 2010). We observed in this study that AC-3E treatment resulted in time-dependent, down-regulation of ER α protein expression, and a series of proteins involved in the PI3K/Akt pathway, such as PI3K, Akt, mTOR in estrogen-dependent T47D breast cancer cells (Fig. 6), suggesting that AC-3E inhibited T47D cell proliferation via blockage of the ER α /PI3K/Akt-mediated signaling pathway. This result may imply that AC-3E can function as an antagonistic agent to estrogen. On the other hand, E-cadherin and β -catenin proteins involved in epithelial-mesenchymal transition, which is essential for cancer cell migration and metastasis, was also regulated by AC-3E treatment. E-cadherin acts as an invasion suppressor of various epithelial malignancies, including breast

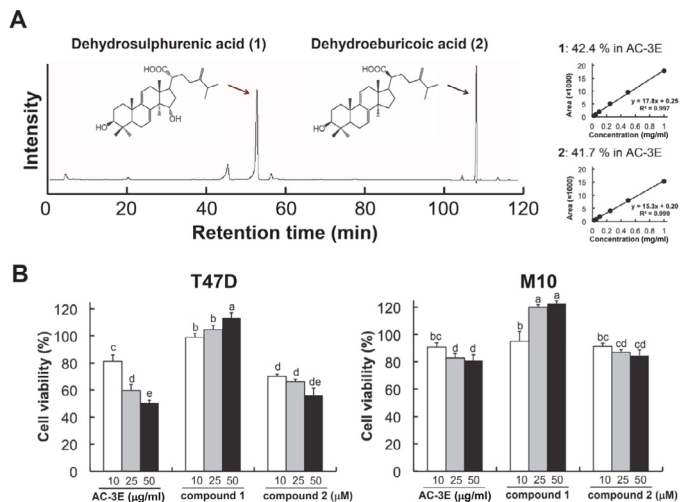


Fig. 9. (A) Chemical fingerprinting of AC-3E and quantification of two major compounds using HPLC analysis. (B) Cytotoxicity assay of compounds 1 and 2 on T47D and M10 cells.

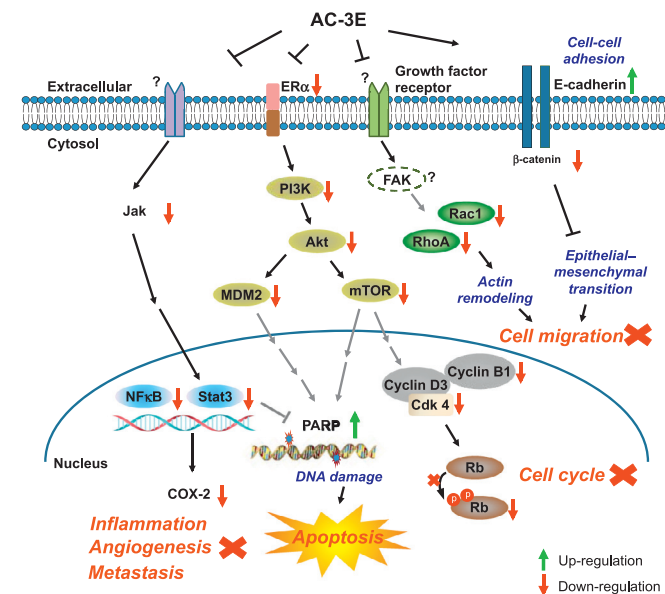


Fig. 10. Summary of the molecular mechanisms of AC-3E proposed to exert anti-breast cancer activity.

cancer (Hirohashi, 1998), while, β -Catenin, a multifunctional protein, mediates cancer cells to be more motile and invasive (Hayashida et al., 2005). The up-regulation and down-regulation of E-cadherin and β -catenin, respectively, by AC-3E present the novel anti-T47D breast cancer cell activity of the extracts.

The Janus kinase (Jak)/signal transducer and activator of transcription 3 (Stat3) pathway is an important mediator of cell inflammation and carcinogenesis. Through activation by growth factors or cytokine receptors, Stat3 upregulates several oncogenic factors, for instance, NF κ B and COX-2, which are important modulators of inflammation, angiogenesis, and metastasis (Yu et al., 2009). The expression of Jak1, Stat3, NF κ B, and COX-2 proteins was reduced in AC-3E-treated T47D cells (Fig. 6), suggesting that the anti-breast cancer cell activity of AC-3 extracts, may in part be through de-regulating the Jak/Stat3 pathway.

Together, schematic mechanisms of AC-3 extracts to exert anti-breast cancer cell activities are proposed (Fig. 10). Firstly, AC-3 extracts inactivate the ER, and subsequently blockage the

PI3K/Akt/mTOR proliferation and survival pathway, which, in turn, inhibits cell cycle progression and induces cell apoptosis. AC-3 extracts may also deregulate the Jak/Stat3 pathway, resulting in inhibition of COX-2 expression. On the other hand, AC-3 extracts exhibit remarkable anti-cancer cell migration activity through suppressing actin remodeling and stress fiber formation, and epithelial-mesenchymal transition via down-regulation of the expression of Rac1, RhoA, and β -catenin, and up-regulation of E-cadherin (Fig. 10).

Accumulating evidence indicates that angiogenesis is an essential process for tumor cell growth and expansion. AC extract may decrease the production of vascular epithelial growth factor (VEGF), a marker of angiogenesis *in vivo* pulmonary metastasis (Chang et al., 2015). In our study, we observed that AC-3E inhibited tube-like structures as compared with control cells in VEGF-stimulated HUVECs (Fig. 5). In addition, the *ex vivo* chick chorioallantoic membrane (CAM) assay results demonstrated the profound anti-angiogenic activity of AC-3E comparable to that of tamoxifen, as microvasculature was markedly reduced (Fig. 7). Moreover, the endothelial cell marker protein CD31 was observed abundantly present in the T47D tumor specimen, indicating tumor angiogenesis (Fig. 8). AC-3E treatment showed a profound effect on suppressing the level of CD31 proteins. The highly proliferative status of T47D cells (highly expressing proliferating marker Ki67) was observed in tumor specimens (tumor control), which was also significantly inhibited in the AC-3E-treated groups. Notably, our T47D tumor xenograft data revealed that among the five treatment groups, the AC-3E-100 and PreAC-3E-50 treatment showed the most significant suppression of tumor growth at 90% and 89% ($P < 0.01$), indicating the novel antitumor activity of AC-3 extracts. Furthermore, the combinational treatment of tumor-bearing mice by Tam-30 and AC-3E-50 showed similar inhibition on tumor growth compared to treatment with Tam-30 only, suggesting that the adverse effect of tamoxifen in stimulating tumor growth or drug resistance in patients might be able to overcome by reducing its intervention doses through combined treatment with AC extracts. Together, we suggest that AC-3 extracts can be used as a double-barreled approach to treat human breast cancer by attacking both the cancer cells as well as tumor-associated blood vessel cells.

Several kinds of compounds, including terpenoids, flavonoids, polysaccharides, polyacetylenes, and benzoquinone derivatives have been identified from the mycelium culture or fruiting bodies of *A. cinnamomea*, and some of the bioactivities of these compounds have been reported (Geethangili and Tzeng, 2011; Yang et al., 2012a; Lin et al., 2011). Camphorataamide B, for example, which was isolated from AC mycelium culture, was reported to inhibit the cell growth, cell cycle progression and tumor growth of triple negative human breast cancer MDA-MB-231 cells (Lin et al., 2012). Antrocin isolated from AC fruiting bodies was reported to lead to MDA-MB-231 cell death through the Akt/mTOR pathway (Rao et al., 2011). However, not much information is available about anti-ER+ breast cancer cell activity. In this study, a significantly high abundance of two lanostane-type triterpenes, namely dehydrosulphurenic acid (1) (42.4%) and dehydroeburicoic acid (2) (41.7%), were identified from AC-3 fruiting body extracts. Both compounds were reported to exert *in vitro* anti-inflammatory and anti-insecticidal activities (Geethangili and Tzeng, 2011). However, we found that only dehydroeburicoic acid (2) exhibited an inhibitory effect on viability of ER positive T47D breast cancer cells. The toxicity of dehydroeburicoic acid treatment is similar to that of AC crude extract prepared from a 3-month-age fruiting body. Du's study showed that dehydroeburicoic acid (2) identified from a triterpenoid-enriched fraction in AC extracts was found to exert potent cytotoxic effect against leukemia (Du et al., 2012). The specific modes of action of dehydroeburicoic acid on breast cancer cells may warrant further investigation.

Author contributions

K. M. S., T. H. S. and L. F. S. designed the research study.
K. M. S., T. H. S., W. L. L., C. Y. C., B. Y. H. and S. Y. W. performed the studies and analyzed the data.
W. W. H. cultivated and collected the AC fruiting body.
K. M. S., T. H. S., W. L. L., and L. F. S. wrote the manuscript.
L. F. S. supervised the research.

Conflict of interest

The authors declare that they have no conflict of interests. The authors declare no competing financial interests.

Acknowledgments

This study was supported by institutional grant funding from Academia Sinica, Taiwan. The authors thank Dr. Jung-Yaw Lin for his support on this project and Mr. Chung-Chih Yang for his technical assistance on the tube formation experiments.

References

- Ahmad, S., Singh, N., Glazer, R.I., 1999. Role of AKT1 in 17 β -estradiol- and 532 insulin-like growth factor I (IGF-I)-dependent proliferation and prevention of apoptosis in MCF-7 breast carcinoma cells. *Biochem. Pharmacol.* 58, 425–430.
- Ao, Z.H., Xu, Z.H., Lu, Z.M., Xu, H.Y., Zhang, X.M., Dou, W.F., 2009. Niuchangchih (*Antrodia camphorata*) and its potential in treating liver diseases. *J. Ethnopharmacol.* 121, 194–212.
- Bratton, M.R., Duong, B.N., Elliott, S., Weldon, C.B., Beckman, B.S., McLachlan, J.A., Burrow, M.E., 2010. Regulation of ERalpha-mediated transcription of Bcl-2 by PI3K-AKT crosstalk: implications for breast cancer cell survival. *Int. J. Oncol.* 37, 541–550.
- Carraway, H., Hidalgo, M., 2004. New targets for therapy in breast cancer: mammalian target of rapamycin (mTOR) antagonists. *Breast Cancer Res.* 6, 219–224.
- Chang, C.H., Huang, T.F., Lin, K.T., Hsu, C.C., Chang, W.L., Wang, S.W., Ko, F.N., Peng, H.C., Chung, C.H., 2015. 4-Acetylantroquinolon B suppresses tumor growth and metastasis of hepatoma cells via blockade of translation-dependent signaling pathway and VEGF production. *J. Agric. Food. Chem.* 63, 208–215.
- Chang, C.W., Chen, C.C., Wu, M.J., Chen, Y.S., Chen, C.C., Sheu, S.J., Lin, T.W., Chou, S.H., Lin, S.C., Liu, C.J., Lee, T.C., Huang, C.Y., Lo, J.F., 2013. Active Component of *Antrodia cinnamomea* Mycelia Targeting Head and Neck Cancer Initiating Cells through Exaggerated Autophagic Cell Death. *Evid. Based Complement Alternat. Med.*, 2013, 946451.
- Chen, Y.Y., Liu, F.C., Chou, P.Y., Chien, Y.C., Chang, W.S., Huang, G.J., Wu, C.H., Sheu, M.J., 2012. Ethanol extracts of fruiting bodies of *Antrodia cinnamomea* suppress CL1-5 human lung adenocarcinoma cells migration by inhibiting matrix metalloproteinase-2/9 through ERK, JNK, p38, and PI3K/Akt signaling pathways. *Evid. Based Complement Alternat. Med.*, 2012, 378415.
- Cheng, P.C., Huang, C.C., Chiang, P.F., Lin, C.N., Li, L.L., Lee, T.W., Lin, B., Chen, I.C., Chang, K.W., Fan, C.K., Luo, T.Y., 2014. Radioprotective effects of *Antrodia cinnamomea* are enhanced on immune cells and inhibited on cancer cells. *Int. J. Radiat. Biol.* 90, 841–852.
- Chung, H., Jung, J.Y., Cho, S.D., Hong, K.A., Kim, H.J., Shin, D.H., Kim, H., Kim, H.O., Shin, D.H., Lee, H.W., Jeong, L.S., Kong, G., 2006. The antitumor effect of IJ-529, a novel agonist to A3 adenosine receptor, in both estrogen receptor-positive and estrogen receptor-negative human breast cancers. *Mol. Cancer Ther.* 5, 685–692.
- Du, Y.C., Chang, F.R., Wu, T.Y., Hsu, Y.M., El-Shazly, M., Chen, C.F., Sung, P.J., Lin, Y.Y., Lin, Y.H., Wu, Y.C., Lu, M.C., 2012. Antileukemia component, dehydroeburicoic acid from *Antrodia camphorata* induces DNA damage and apoptosis *in vitro* and *in vivo* models. *Phytomedicine* 19, 788–796.
- Geethangili, M., Tzeng, Y.M., 2011. Review of pharmacological effects of *Antrodia camphorata* and its bioactive compounds. *Evid. Based Complement Alternat. Med.* 212641.
- Hall, A., Nobes, C.D., 2000. Rho GTPases: molecular switches that control the organization and dynamics of the actin cytoskeleton. *Philos. Trans. R. Soc. Lond., B, Biol. Sci.* 355, 965–970.
- Hayashida, Y., Honda, K., Idogawa, M., Ino, Y., Ono, M., Tsuchida, A., Aoki, T., Hirohashi, S., Yamada, T., 2005. E-cadherin regulates the association between beta-catenin and actinin-4. *Cancer Res.* 65, 8836–8845.
- Hirohashi, S., 1998. Inactivation of the E-cadherin-mediated cell adhesion system in human cancers. *Am. J. Pathol.* 153, 333–339.
- Hseu, Y.C., Chen, S.C., Chen, H.C., Liao, J.W., Yang, H.L., 2008. *Antrodia camphorata* inhibits proliferation of human breast cancer cells *in vitro* and *in vivo*. *Food Chem. Toxicol.* 46, 2680–2688.
- Hseu, Y.C., Chen, S.C., Tsai, P.C., Chen, C.S., Lu, F.J., Chang, N.W., Yang, H.L., 2007. Inhibition of cyclooxygenase-2 and induction of apoptosis in estrogen-nonresponsive breast cancer cells by *Antrodia camphorata*. *Food Chem. Toxicol.* 45, 1107–1115.

- Hseu, Y.C., Yang, H.L., Lai, Y.C., Lin, J.G., Chen, G.W., Chang, Y.H., 2004. Induction of apoptosis by *Antrodia camphorata* in human premyelocytic leukemia HL-60 cells. *Nutr. Cancer* 48, 189–197.
- Hsu, Y.L., Kuo, P.L., Cho, C.Y., Ni, W.C., Tzeng, T.F., Ng, L.T., Kuo, Y.H., Lin, C.C., 2007. *Antrodia cinnamomea* fruiting bodies extract suppresses the invasive potential of human liver cancer cell line PLC/PRF/5 through inhibition of nuclear factor kappaB pathway. *Food Chem. Toxicol.* 45, 1249–1257.
- Huang, C.H., Chang, Y.Y., Liu, C.W., Kang, W.Y., Lin, Y.L., Chang, H.C., Chen, Y.C., 2010. Fruiting body of *Niuchangchih* (*Antrodia camphorata*) protects livers against chronic alcohol consumption damage. *J. Agric. Food Chem.* 58, 3859–3866.
- Kim, J., Yu, W., Kovalski, K., Ossowski, L., 1998. Requirement for specific proteases in cancer cell intravasation as revealed by a novel semiquantitative PCR-based assay. *Cell* 94, 353–362.
- Lee, W.L., Shyur, L.F., 2012. Deoxyelephantopin impedes mammary adenocarcinoma cell motility by inhibiting calpain-mediated adhesion dynamics and inducing reactive oxygen species and aggresome formation. *Free Radic. Biol. Med.* 52, 1423–1436.
- Lin, T.Y., Chen, C.Y., Chien, S.C., Hsiao, W.W., Chu, F.H., Li, W.H., Lin, C.C., Shaw, J.F., Wang, S.Y., 2011. Metabolite profiles for *Antrodia cinnamomea* fruiting bodies harvested at different culture ages and from different wood substrates. *J. Agric. Food Chem.* 59, 7626–7635.
- Lin, W.L., Lee, Y.J., Wang, S.M., Huang, P.Y., Tseng, T.H., 2012. Inhibition of cell survival, cell cycle progression, tumor growth and cyclooxygenase-2 activity in MDA-MB-231 breast cancer cells by camphorataimide B. *Eur. J. Pharmacol.* 680, 8–15.
- Rao, Y.K., Fang, S.H., Tzeng, Y.M., 2007. Evaluation of the anti-inflammatory and anti-proliferation tumoral cells activities of *Antrodia camphorata*, *Cordyceps sinensis*, and *Cinnamomum osmophloeum* bark extracts. *J. Ethnopharmacol.* 114, 78–85.
- Rao, Y.K., Wu, A.T., Geethangili, M., Huang, M.T., Chao, W.J., Wu, C.H., Deng, W.P., Yeh, C.T., Tzeng, Y.M., 2011. Identification of antrocin from *Antrodia camphorata* as a selective and novel class of small molecule inhibitor of Akt/mTOR signaling in metastatic breast cancer MDA-MB-231 cells. *Chem. Res. Toxicol.* 24, 238–245.
- Ring, A., Dowsett, M., 2004. Mechanisms of tamoxifen resistance. *Endocr. Relat. Cancer* 11, 643–658.
- Schafer, J.M., Lee, E.S., O'Regan, R.M., Yao, K., Jordan, V.C., 2000. Rapid development of tamoxifen-stimulated mutant p53 breast tumors (T47D) in athymic mice. *Clin. Cancer Res.* 6, 4373–4380.
- Sepp, K.J., Auld, V.J., 2003. RhoA and Rac1 GTPases mediate the dynamic rearrangement of actin in peripheral glia. *Development* 130, 1825–1835.
- Yang, H.L., Chen, C.S., Chang, W.H., Lu, F.J., Lai, Y.C., Chen, C.C., Hseu, T.H., Kuo, C.T., Hseu, Y.C., 2006. Growth inhibition and induction of apoptosis in MCF-7 breast cancer cells by *Antrodia camphorata*. *Cancer Lett.* 231, 215–227.
- Yang, H.L., Kuo, Y.H., Tsai, C.T., Huang, Y.T., Chen, S.C., Chang, H.W., Lin, E., Lin, W.H., Hseu, Y.C., 2011. Anti-metastatic activities of *Antrodia camphorata* against human breast cancer cells mediated through suppression of the MAPK signaling pathway. *Food Chem. Toxicol.* 49, 290–298.
- Yang, H.L., Kumar, K.J.S., Hseu, Y.C., 2012a. Multiple molecular targets of *Antrodia camphorata*: a suitable candidate for breast cancer chemoprevention. In: Aft, Rebecca (Ed.), *Targeting New Pathways and Cell Death in Breast Cancer*. InTech, pp. 158–180.
- Yang, H.W., Shin, M.G., Lee, S., Kim, J.R., Park, W.S., Cho, K.H., Meyer, T., Heo, W.D., 2012b. Cooperative activation of PI3K by Ras and Rho family small GTPases. *Mol. Cell* 47, 281–290.
- Yu, H., Pardoll, D., Jove, R., 2009. STATs in cancer inflammation and immunity: a leading role for STAT3. *Nat. Rev. Cancer* 9, 798–809.